Short-wave Infrared Colloidal Quantum Dot Photodetectors on Silicon

Chen Hu*[a, b, c], Alban Gassenq[a, b], Yolanda Justo[c], Sergii Yakunin[d], Wolfgang Heiss[d], Zeger Hens[c], Gunther Roelkens[a, b]

[a] Photonics Research Group, INTEC Department, Ghent University-IMEC, Sint-Pietersnieuwstraat 41, 9000 Ghent, Belgium

[b] Center for Nano- and Biophotonics (NB-Photonics), Ghent University, Belgium

[c] Physics and Chemistry of Nanostructures, Ghent University, Krijgslaan 281-S3, 9000 Gent, Belgium;

[d] Institute for Semiconductor and Solid State Physics, Johannes Kepler University of Linz, Altenbergerstr. 69, 4040 Linz, Austria

ABSTRACT

In this paper, two kinds of colloidal quantum dots, PbS and HgTe, are explored for SWIR photodetectors application. The colloidal dots are prepared by hot injection chemical synthesis, with organic ligands around the dots keeping them stable in solution. For the purpose of achieving efficient carrier transport between the dots in a film, these long organic ligands are replaced by shorter, inorganic ligands. We report uniform, ultra-smooth colloidal QD films without cracks realized by dip-coating and corresponding ligand exchange on a silicon substrate. Metal-free inorganic ligands, such as OH^- and S^{2-}, are investigated to facilitate the charge carrier transport in the film. Both PbS and HgTe-based quantum dot photoconductors were fabricated on interdigitated gold electrodes. For PbS-based detectors a responsivity of 200A/W is measured at 1.5µm, due to the large internal photoconductive gain. A 2.2µm cut-off wavelength for PbS photodetectors and 2.8µm for HgTe quantum dot photodetectors are obtained.

Keywords: colloidal quantum dots, solid-state ligand exchange, photoconductor

1. INTRODUCTION

Many molecules that we want to detect in our environment have bands of absorption lines in the short-wave infrared (SWIR). Traditional high-sensitivity photodetectors used in these spectroscopic systems are discrete components based on epitaxial materials[1-2]. However, the size of these systems makes them hard to be deployed in the field. On the other hand, while the III-V semiconductor leads to the highest performance, the high material and integration cost prohibits large volume application. Low-cost MidIR photodetectors based on colloidal quantum dots (QDs) offer an alternative way to realize this functionality, either as discrete components or integrated on photonic integrated circuits[3-5].

Using colloidal QDs as new photonic materials gets a lot of attention in the photonic community. The simple hot injection chemical synthesis method allows low-cost production[6-7]. By tuning the size of the QDs, the electrical and optical properties (such as the absorption cut-off wavelength) can be tuned due to the quantum size effect[8]. Furthermore, the fact that these QDs are available in solution makes it easy to do large-area heterogeneous integration on substrates, using dip coating or printing, which can offer a considerable cost reduction as compared to thermal evaporation or epitaxially grown layer stacks[9].

Therefore, in this paper we investigate the use of two kinds of colloidal quantum dot materials, PbS and HgTe, for short-wave infrared photodetector application. We demonstrate a uniform, ultra-smooth colloidal QD film without any cracks, which is realized by dip coating and subsequent ligand exchange. Metal-free inorganic ligands, such as OH^- and S^{2-}, are investigated to facilitate the charge carrier transport[10]. For PbS QD photodetectors, devices are fabricated by dip coating on prefabricated interdigitated electrodes. The HgTe QD photodetector is produced by a one step drop casting process with corresponding ligand exchange.

*chenhu@intec.ugent.be; phone 0032(0)489 235 363

2. EXPERIMENTAL SECTION

2.1 PbS QD synthesis and ligand exchange

The PbS QD synthesis is based on the procedure of Iwan Moreels *et al* [6,8]. A stock solution of 0.16 g (5mmol) S dissolved in 15mL of oleylamine (OlAm, C18-content 80-90%) is prepared by heating the mixture under nitrogen for 30 min at 120 ºC. For the synthesis, 0.834g (3 mmol) of $PbCl_2$ and 7.5 mL of OlAm is used in a three-neck flask. This mixture is degassed for 30 min under nitrogen at 125 ºC. Afterwards the $PbCl_2$ solution is heated up to the required injection temperature, and then 2.25 mL of the OlAm-S stock solution (0.75 mmol of S) and 170 µL (375 µmol, half of the amount of S) of tri-n-octylphosphine (TOP) are injected into the flask. The temperature drops approximately 5-10 ºC, and the resulting growth temperature is maintained throughout the reaction. After the designed growth time, the reaction is quenched by adding 10 mL of toluene and 15 mL of MeOH. After centrifugation of the suspension and decantation of the supernatant, the PbS QDs are resuspended in 10 mL of toluene. For the PbS QDs studied in this paper, the growth temperature is 160 ºC and the growth time is 2 hour 30 min.

After synthesis, the PbS QDs can not be precipitated and resuspended more than once due to a loss of ligands and subsequent QDs clustering. The OlAm ligand can however easily be replaced by oleic acid (OlAc). An exchange OlAc is typically realized by adding OlAc to a toluene suspension of PbS QDs in a ratio of 1.5:10 OlAc/toluene. After precipitation with methanol (MeOH) and centrifugation, the QDs are resuspended in toluene and the exchange is repeated. Finally the QDs can be precipitated once more with MeOH to remove excess OlAc and resuspended in toluene.

In order to characterize the PbS QDs, the sizing curve developed by Iwan Moreels *et al* [6] is used, which enables to determine the quantum dot size *d* (nm) directly from the spectral position of the first exciton absorption peak.

$$E_0 = 0.41 + \frac{1}{0.0252d^2 + 0.283d} \tag{1}$$

Furthermore, the QD molar extinction coefficient ε at 400 nm can be determined.

$$\varepsilon_{400} = 0.0234d^3 \,\mathrm{cm}^{-1}/\mu\mathrm{M} \tag{2}$$

With Beer's Law

$$A = \varepsilon \cdot c_0 \cdot L \quad (L \text{ is the sample length}) \tag{3}$$

the QD concentration c_0 can be calculated directly from the absorbance at 400 nm A_{400} and QD molar extinction coefficient ε at 400 nm. Samples for absorbance spectroscopy are prepared by drying a known volume of the QD solution with nitrogen and resuspending them in tetrachloroethylene (C_2Cl_4).

2.2 HgTe QD synthesis and ligand exchange

Dodecanethiol-capped HgTe QDs are prepared on the procedure of Maksym V. Kovalenko *et al* [7]. Thoiglycerol stabilized HgTe QDs were synthesized in aqueous solution using the precipitation reaction of hydrogen telluride gas and mercury perchlorate. Hereafter, a phase-transfer procedure from aqueous solution to nonpolar organic solvents was carried out via the ligand exchange with dodecanethiol. In order to realize the purification, the dodecanethiol-capped HgTe QDs are resuspended in anhydrous hexane and precipitated with MeOH as solvent/non-solvent pair twice and filtering the HgTe QDs through 0.2µm PTFE filter. Finally, the HgTe QDs are resuspended in chlorobenzene.

2.3 PbS QD thin film preparation and solid state ligand exchange

The PbS QD thin film is prepared by dip coating an intrinsic Si substrate into a 1 µM PbS QDs suspension in toluene with 80 mm/min dipping speed. Afterwards, the PbS QD film is re-immersed into the metal free ligand exchange solution. After the desired ligand exchange time, formamide, acetone and isopropanol is used to remove excess exchange solution and the sample is dried under nitrogen. The dipping procedure with solid-state ligand exchange can be done repetitively to implement a multi-layer film. In order to realize solid-state ligand exchange with S^{2-} and OH^-, 10 mg/mL $Na_2S{\cdot}9H_2O$ suspended in formamide (FA) and 0.01 mg/mL KOH in FA solution is used respectively.

2.4 Photodetector fabrication

The PbS photodetector is prepared in a way similar to the PbS thin film. The process starts with the deposition of an insulating SiO_2 layer by plasma enhanced chemical vapor deposition (PECVD). Afterwards a pair of interdigitated finger

electrodes are defined by a lift-off process, consisting of 10 nm Ni and 100 nm Au. The electrodes are designed with 2 µm wide fingers with 2 µm separation between them attached to two independent contact pads (shown in Figure 1 (a)).

The HgTe photodetector is prepared by drop casting a 0.2 µL dodecanethiol-capped HgTe suspension in chlorobenzene on a gold electrode pattern. The sample contains a pair of finger shaped gold electrodes (the pattern is defined by lithography and metal lift-off) on a glass substrate. The distance between the two fingers is 15 µm and the active area of the detector is 15 µm * 8 mm (shown in Figure 1(b)). For the purpose of solid-state ligand exchange, 0.01 mg/mL KOH in FA solution is directly dropped on the film for 10 seconds and afterwards rinsed with the same recipe for PbS ligand exchange.

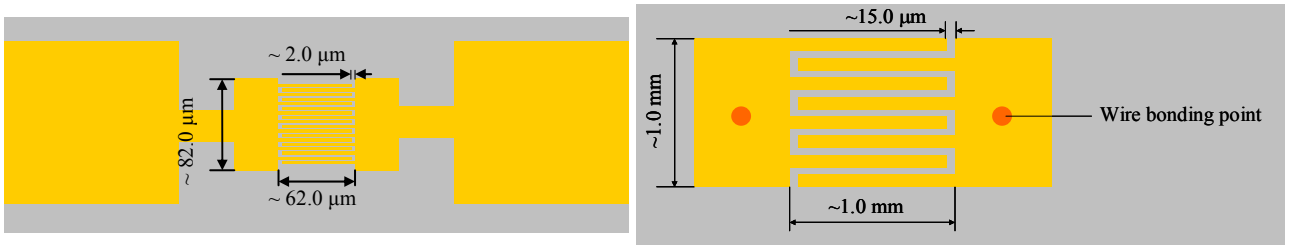

(a) (b)

Figure 1. Illustration of (a) PbS and (b) HgTe detector electrodes design (top view)

3. RESULTS AND DISCUSSION

3.1 PbS QD synthesis

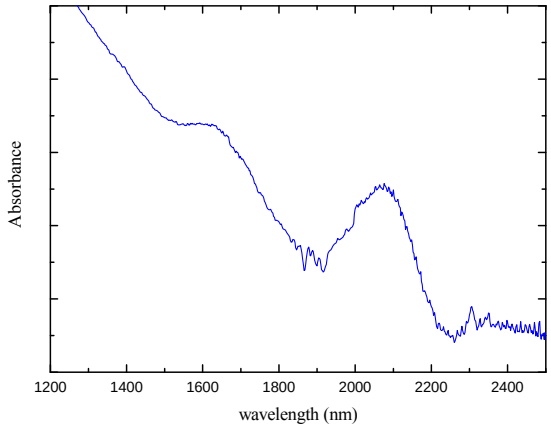

Figure 2. Absorbance spectra of PbS QD suspensions in the short-wave infrared, synthesized at 160 ºC with a total growth time of 2 hour 30 min.

Figure 2 shows a typical absorbance spectrum with a first exciton transition peak in the short-wave infrared range, illustrating a cut-off wavelength of 2.2 µm. The quantum dot size is about 10 nm according to the sizing curve. According to Beer's Law, the concentration is about 2.106 µMol/L.

3.2 Solid state ligand exchange of PbS QD film

According to the absorbance spectra, PbS QDs can be used to achieve interband transitions up to 2.2 µm. Thus we can realize photodetectors based on such colloidal QDs on silicon or on silicon waveguide circuits with solution-based processes, e.g. drop casting, spin coating, printing, etc. Nevertheless, the electrically insulating organic ligand shells existing in the as-deposited QD film prohibits charge carrier transport in the film and therefore they need to be removed to obtained photoconductive devices. For this purpose, a solid-state metal free ligand exchange process is used to remove the organic surrounding QDs. An FTIR is used to monitor the effect of ligand exchange treatments.

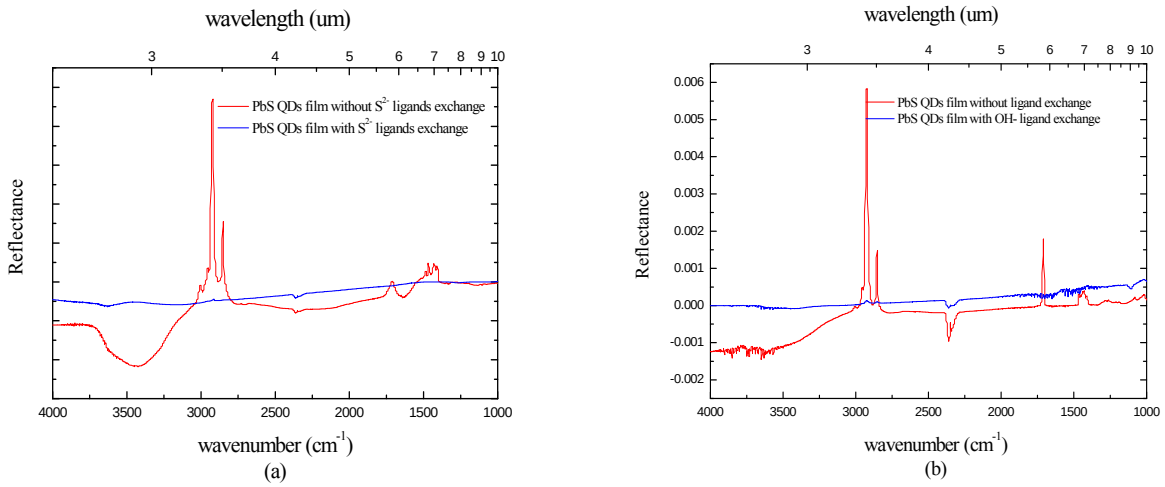

Figure 3. (a) Reflection- Fourier Transform InfraRed (FTIR) spectra of OlAc-capped PbS colloidal QD film and S^{2-} -capped PbS colloidal QD film after $Na_2S{\cdot}9H_2O$ treatment. (b) Reflection-FTIR spectra of OlAc-capped PbS colloidal QD film and OH^--capped PbS colloidal QD film after KOH treatment.

Figure 3 (a) compares the reflection-FTIR spectra of OlAc-capped PbS colloidal QD film and S^{2-} -capped PbS colloidal QD film after $Na_2S{\cdot}9H_2O$ treatment. After the treatment, the C = C stretching peak around 3010 cm^{-1}, $-CH_2$ asymmetric stretching at 2920 cm^{-1} and $-CH_3$ symmetric stretching at 2850 cm^{-1} no longer exists, which indicates that most of the organic ligands are removed. Figure 3 (b) shows similar results for KOH treatment, showing also that most of the organics are removed from the QD film.

The ligand exchange induces a clustering of the nanoparticles due to the removal of the long ligands. This is a main challenge that needs to be addressed, since resulting cracks in the QD film will prevent charge carrier transport. In this paper, multiple times dip coating with solid state ligand exchange is used to overcome this issue.

Figure 4 (a), (b), (c) show the surface morphology of a PbS QD film deposited by of 6 time dipping without chemical treatment, with $Na_2S{\cdot}9H_2O$ treatment and KOH treatment, respectively. After chemical treatment, Figure 4 (b) and (c) reveal clearly a reduction of interparticle spacing, which results in a mobility increase of the film. Specifically, compared with KOH treatment, the $Na_2S{\cdot}9H_2O$ treated film exhibits more close packaging of the QDs. This corresponds well with the optoelectronic characterization results, as will be discussed later. Moreover, the film morphology after treatment illustrates that a crack-free and homogenous film can be implemented, which is suitable for optoelectronic applications.

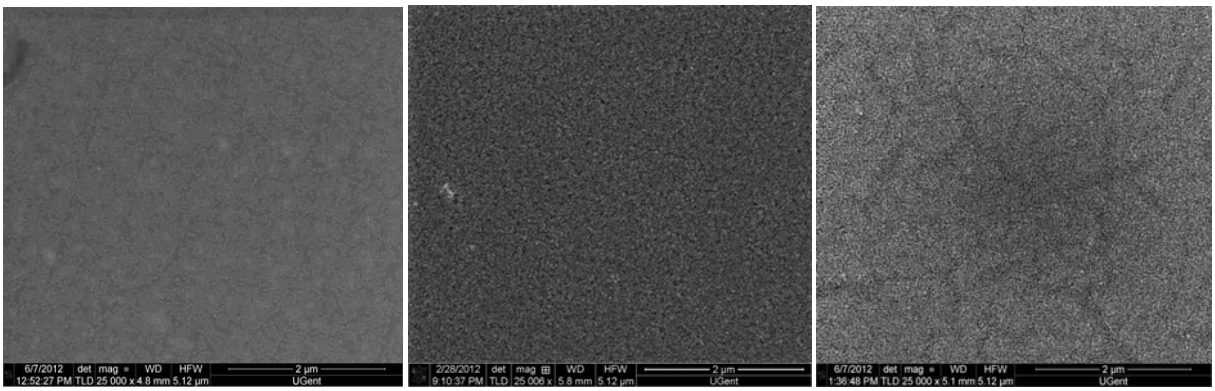

Figure 4. Scanning electron microscope (SEM) images of (a) OlAc-capped PbS colloidal QD film (b) S^{2-} -capped PbS colloidal QD film (c) OH^- -capped PbS colloidal QD film.

3.3 PbS Photodetector characterization

The current-voltage characteristics of PbS photoconductive photodetectors is done by surface illumination with a fiber coupled near infrared SLED (λ ~ 1.55 μm). Figure 5 presents the I-V characteristics as a function of incident optical power. Under illumination, the resistance of S^{2-} capped PbS QD photodetector increases from a dark resistivity of 2.67 kΩ to 1.22 kΩ at 10 V bias under 16 mW optical illumination; the OH- capped PbS photodetector shows a similar trend from dark resistivity of 7.35 kΩ to 1.57 kΩ under the same illuminate condition. The OH^- capped PbS colloidal QD detector shows an lower conductivity compared to S^{2-} capped PbS QD detector, which corresponds to the more close packing of S^{2-} capped PbS QDs after ligand exchange.

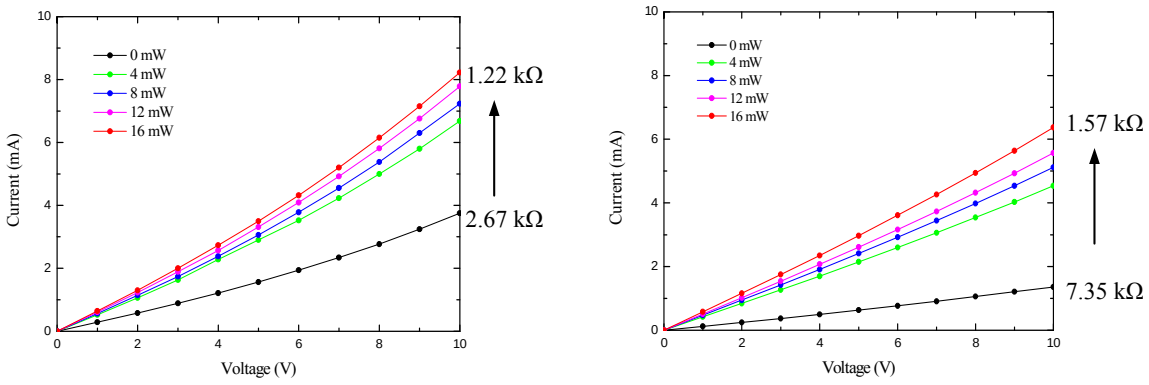

Figure 5. Current-voltage characteristics of processed (a) S^{2-} capped PbS (b) OH^- capped PbS colloidal QD photoconductive photodetectors.

Figure 6 shows the responsivity of OH^- capped PbS QD detector as a function of illumination power level. The curve exhibits an increase of responsivity with decreasing illumination. For 500 nW illumination power with 10 V bias, the responsivity can reach more than 200 A/W. This rather high value implies a high internal photoconductive gain, which is due to the long carrier lifetime compare to the carrier transit time. These long lifetime carrier result from the trap states inside the QD thin film. With the increase of illumination power, the long-lived trap states will be filled and consequently a lower gain will result.

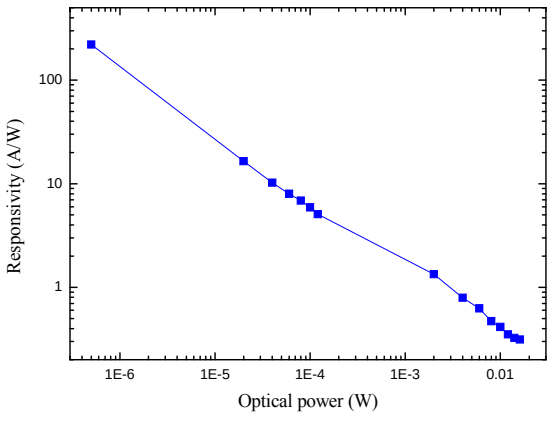

Figure 6. Responsivity dependence as a function of optical power at 1.55 μm and a bias voltage of 10 V for an OH^- -capped PbS colloidal QD photodetector.

FTIR-based calibration measurements are used to get the spectral response of the PbS photodetector[11]. An internal tungsten halogen source in the FTIR spectrometer is modulated by a Michelson interferometer and is used to illuminate the photodetector with a set of gold mirrors. The photoconductor is driven by 0.3 mA current and the resultant voltage drop signal is send back to the FTIR electrical input to calculate the spectral dependence of the responsivity (in arbitrary units). The normalized detector responsivities as a function of wavelength for PbS QD photodetector is presented in Figure 7. The two spectral response curves illustrate that the first transition peak of PbS QDs (around 2.0 μm) still exists after ligand exchange, and photodetection up to 2.2 μm can be achieved.

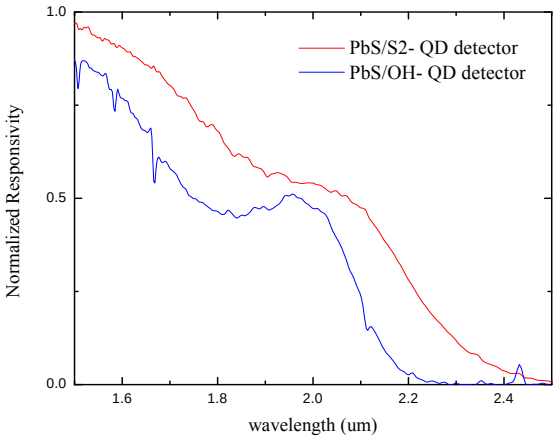

Figure 7. Normalized detector responsivity as a function of wavelength for S^{2-} capped and OH^- capped PbS QD photodetector.

3.4 HgTe Photodetector characterization

For the HgTe photodetector, an incandescent light / monochromator combination is used to acquire current-voltage characteristics and spectral response curve. The normalized current-voltage characteristics of the HgTe photodetector can be seen in Figure 8, in order to compare HgTe photodetectors and PbS devices. The PbS contrast sample is prepared by drop casting 0.2 μL OlAc-capped PbS suspended in toluene on a gold electrode pattern, after which 0.01 mg/mL KOH in FA solution is drop casted on the film for 10 seconds ligand exchange, after which the sample is rinsed to remove excess KOH.

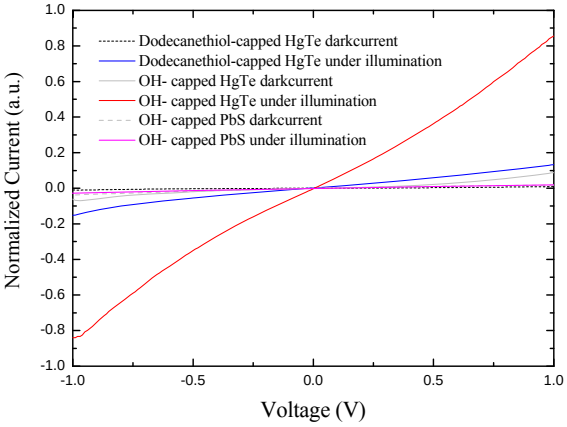

Figure 8. Current-voltage characteristics of processed HgTe and PbS photoconductive detectors.

The graph illustrates that the HgTe colloidal quantum dots exhibit much higher photosensitivity compared to PbS. Also, the measurements show that OH- capped HgTe QDs outperform dodecanethiol-capped HgTe QDs, which is most likely related to the shorter ligand length in the first case.

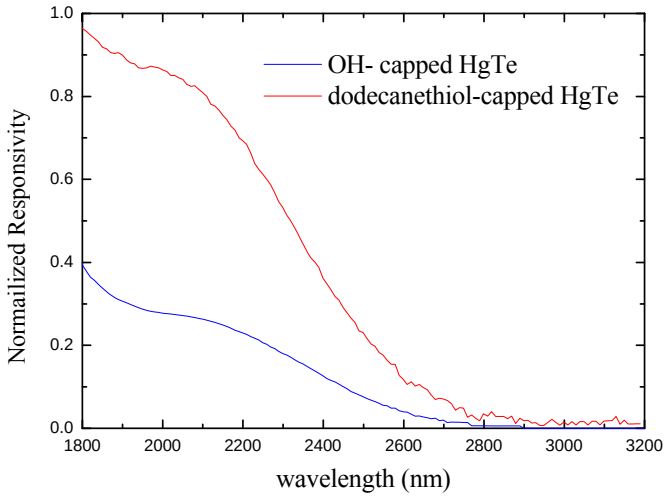

Figure 9. normalized spectral response of dodecanethiol-capped and OH- capped HgTe QD photoconductive photodetectors.

The normalized spectral response curves of HgTe photodetector is presented in Figure 9. Both curves illustrate that HgTe detectors are useful for near-infrared and mid-infrared photodetection. The higher responsivity of OH- capped HgTe QD detector reveals that metal-free ligand exchange method is promising to improve the detector performance.

4. CONCLUSIONS

In this paper, two kinds of colloidal quantum dot material, PbS and HgTe, are explored for SWIR photodetector applications. We have demonstrated a uniform, ultra-smooth colloidal QD film without cracks by dip coating and subsequent ligand exchange. Metal-free inorganic ligands, such as OH- and S2- are investigated to facilitate the charge carrier transport. PbS photoconductors with a responsivity of 200A/W are obtained at 1.5μm (cut-off wavelength 2.2μm). We also show that HgTe photodetectors with a cut-off wavelength of 2.8μm can be realized by metal free ligand exchange, with improved performance compared to PbS detectors. The integration of these photodetectors on silicon waveguide circuits will be discussed during the conference.

ACKNOWLEDGEMENT

This work is supported by the FWO-NanoMIR project and the FP7-ERC-MIRACLE project. We acknowledge the assistance from Steven Verstuyft during the device fabrication. We also acknowledge the assistance from Liesbet Van Landschoot and Kasia Komorowska during SEM measurement.

REFERENCES

[1] Baile Chen, W. Y. Jiang, Jinrong Yuan, Archie L. Holmes, Jr, and Bora. M. Onat, “Demonstration of a room-temperature InP-based photodetector operating beyond 3 μm”, Photonics Technology Letters, Volume 23, Issue 4, 218–220 (2011).

[2] E Plis, J B Rodriguez, G Balakrishnan, Y D Sharma, H S Kim, T Rotter and S Krishna, “Mid-infrared InAs/GaSb strained layer superlattice detectors with nBn design grown on a GaAs substrate”, Semicond. Sci. Technol., 25, 085010 (2010).
[3] Gerasimos Konstantatos, Ian Howard, Armin Fischer, Sjoerd Hoogland, Jason Clifford, Ethan Klem, Larissa Levina1 & Edward H. Sargent, “Ultrasensitive solution-cast quantum dot photodetectors”, Nature 442, 180-183 (2006).
[4] Gerasimos Konstantatos and Edward H. Sargent, “Nanostructured materials for photon detection”, Nature Nanotechnology 5, 391–400 (2010).
[5] Krisztina Szendrei, Fabrizio Cordella, Maksym V. Kovalenko, Michaela Bo¨berl, Gu¨nther Hesser, Maksym Yarema, Dorota Jarzab, Oleksandr V. Mikhnenko, Agnieszka Gocalinska, Michele Saba, Francesco Quochi, Andrea Mura, Giovanni Bongiovanni, Paul W. M. Blom, Wolfgang Heiss, and Maria Antonietta Loi, “Solution-Processable Near-IR Photodetectors Based on Electron Transfer from PbS Nanocrystals to Fullerene Derivatives”, Advanced Materials, Volume 21, Issue 6, 683–687 (2009).
[6] Iwan Moreels, Yolanda Justo, Bram De Geyter, Katrien Haustraete, José C. Martins, and Zeger Hens, “Size-Tunable, Bright, and Stable PbS Quantum Dots: A Surface Chemistry Study”, ACS Nano, 5 (3), pp 2004–2012 (2011).
[7] Maksym V. Kovalenko, Erich Kaufmann, Dietmar Pachinger, Jürgen Roither, Martin Huber, Julian Stangl, Günter Hesser, Friedrich Schäffler, and Wolfgang Heiss, “Colloidal HgTe Nanocrystals with Widely Tunable Narrow Band Gap Energies: From Telecommunications to Molecular Vibrations”, J. Am. Chem. Soc., 128 (11), pp 3516–3517 (2006).
[8] Iwan Moreels, Karel Lambert, Dries Smeets, David De Muynck, Tom Nollet, José C. Martins, Frank Vanhaecke, Andre´ Vantomme, Christophe Delerue, Guy Allan and Zeger Hens, “Size-Dependent Optical Properties of Colloidal PbS Quantum Dots”, ACS Nano Vol. 3(10), 3023–3030 (2009).
[9] Michaela Böberl, Maksym V. Kovalenko, Stefan Gamerith, Emil J. W. List, and Wolfgang Heiss, “Inkjet-Printed Nanocrystal Photodetectors Operating up to 3 μm Wavelengths”, Adv. Mater. 19, 3574–3578 (2007).
[10] Angshuman Nag, Maksym V. Kovalenko, Jong-Soo Lee, Wenyong Liu, Boris Spokoyny, and Dmitri V. Talapin, “Metal-free Inorganic Ligands for Colloidal Nanocrystals: S^{2-}, HS^{-}, Se^{2-}, HSe^{-}, Te^{2-}, HTe^{-}, $TeS3^{2-}$, OH^{-}, and NH^{2-} as Surface Ligands”, J. Am. Chem. Soc. 133, 10612–10620 (2011).
[11] A. Gassenq, F. Gencarelli, J. Van Campenhout, Y. Shimura, R. Loo, G. Narcy, B. Vincent, G. Roelkens, “GeSn/Ge heterostructure short-wave infrared photodetectors on silicon”, submitted for publication.